Available online at www.sciencedirect.com
SCIENCE DIRECT
Polymer 47 (2006) 3915–3921
polymer
www.elsevier.com/locate/polymer

Matrix mediated alignment of single wall carbon nanotubes in polymer composite films

V.N. Bliznyuk [a,*], S. Singamaneni [a], R.L. Sanford [b], D. Chiappetta [b], B. Crooker [b], P.V. Shibaev [b,*]

[a] *Materials Science and Engineering Department, Western Michigan University, Kalamazoo, MI 49008, USA*
[b] *Department of Physics, Fordham University, Bronx, NY 10458, USA*

Received 13 January 2006; received in revised form 16 March 2006; accepted 17 March 2006
Available online 18 April 2006

Abstract

Alignment of single wall carbon nanotubes (SWNT) in liquid crystalline (LC) polymer matrix imparting orientation to the nanotubes along the nematic director was studied by atomic force microscopy, measurements of electrical conductivity and Raman spectroscopy of the composite in the directions parallel and perpendicular to the nematic director. The composites were prepared through dispersion of SWNT with LC monomer in a common solvent, their alignment in nematic monomer and consequent UV polymerization of the monomer. The anisotropy of electrical and optical properties of the system depends strongly on the concentration of the nanotubes in the range of 1–10% SWNT being especially strong for smaller concentrations and negligible at higher loads. A simple semi-quantitative model is suggested to account for the orientational behavior of nanotubes in nematic matrices. It successfully describes the observed anisotropy of physical properties at microscale (up to 200 μm) in terms of anchoring of the polymer chains to the nanotubes surface and adjustment of the nanotubes orientation to the nematic direction due to such coupling. The increasing disorientation of the nematic domains at higher nanotubes loads is explained as a development of larger number of LC defects induced by the nanotubes in the nematic matrix due to their intrinsic nature of aggregation. The anisotropy of physical properties at macro scale (several millimeters) is much smaller and less dependable on SWNT concentration because differently oriented LC domains effectively wash out the anisotropy.

Keywords: Liquid crystalline polymers; Single wall carbon nanotubes; Atomic force microscopy

1. Introduction

Carbon nanotubes are considered as highly prospective filler materials for future polymer composites due to the large surface to volume ratio, high mechanical strength and extraordinary electrical properties [1–3]. For a long time intrinsic conducting polymers (ICP) like polyaniline (PANI) and their composites have been considered as the only choice in the field of flexible electronics [4]. However, due to their poor processability, low stability and prohibitive cost alternate materials are imperative. Polymer composites with tunable electric properties are an important alternative to meet the demands of flexible electronics. Single wall carbon nanotubes, which exhibit metallic and semi-conducting properties depending on their chirality are a natural choice for developing new polymer composites. However, due to the size of carbon nanotubes and significant intertube van der Waals interactions, the synthesis of polymer/nanotube composites with desired distribution and tailored properties (isotropic or anisotropic) has been a significant challenge. Dispersion of carbon nanotubes has been previously achieved by choosing the right solvent [5] for nanotubes and polymer, applying high shear forces and functionalizing carbon nanotubes in order to improve the compatibility with the matrix. Carbon nanotubes have also been dispersed in the polymer matrix by polymerization of the monomer in the presence of a filler [6].

In order to tune the electronic properties (i.e. conductivity) of the composite it is desirable to achieve significant control over the orientation of the carbon nanotubes in the matrix. The orientation of carbon nanotubes has been controlled by a variety of methods including alignment in the presence of strong electric and magnetic fields, mechanical stretching, shear forces, and fluid flow [7–11]. Recently, the alignment of carbon nanotubes in layer-by-layer assembled polyelectrolyte

* Corresponding authors.
E-mail addresses: valery.bliznyuk@wmich.edu (V.N. Bliznyuk), shibpv@yahoo.com (P.V. Shibaev).

0032-3861/$ - see front matter © 2006 Elsevier Ltd. All rights reserved.
doi:10.1016/j.polymer.2006.03.072

films was achieved by blowing air at the air–water interface and inducing the evaporation of the solvents [12]. In all the methods demonstrated so far an 'external force' producing the orientation of the nanotubes has been a common factor.

Anisotropic distribution of SWNT in the polymer matrices results in conductivity increased by several orders of magnitude compared to the isotropic distribution and causes a significant alteration of percolation thresholds [13,14]. Polymer composites of polyvinyl alcohol with less than 1% of multi-walled carbon nanotubes (MWNT) have an increased Young's modulus by a factor of two [15]. This was attributed to the formation of a well-ordered polymer coating, which served as the interface layer between the nanotubes and the matrix.

Liquid crystals (LCs) are expected to have the ability to impose anisotropic order on carbon nanotubes dispersed in a LC matrix. Dierking et al. [7] have recently demonstrated that CNT aggregated into anisotropic fibrils could be aligned resulting in significant anisotropy of the electrical conductivity. However, the anisotropy was higher in the case of MWNT than in the case of SWNT.

In this communication, we describe a novel alignment method using a liquid crystalline polymer matrix as a source of the alignment of the SWNT, obviating any need for strong external forces.

We study the anisotropy of nanotubes' alignment at different concentrations of carbon nanotubes in the matrix and quantify the anisotropy of electrical conductivity in terms of a simple model.

2. Experimental details

The structure of LC monomers used in preparation of oriented LC films is shown in Scheme 1. The LC mixture contained 28% of molecules A (bifunctional cross-linking mesogens), 70% of molecules B (monofunctional mesogenic units), and 2% of benzophenone (the initiator of polymerization). This composition was previously optimized to achive relatively low melting temperature and satisfactory range of the mesogenic (nematic) phase [16].

The nematic phase of the mixture exists in the temperature interval between 55 and 95 °C. The commercial mixture of LC monomers, RMM34 provided by Merck was also used to prepare some films. Physical properties such as electrical conductivity and optical anisotropy of films prepared from both mixtures were very similar. SWNT prepared by the arc discharge process with nickel and yttrium as the catalyst, were donated by Carbolex Inc. and were used without further purification. AFM studied showed that nanotubes are characterized by average diameter of 1.4 nm and are bound into bundles of typically seven nanotubes as reported elsewhere [5].

Carbon nanotubes were mixed with monomers, stirred in a mixture, and heated above the melting temperature. Organic solvent (toluene, Aldrich) was added to the mixture of nanotubes and monomers in order to decrease a viscosity of the mixture. The solution was cast on glass substrates with the deposited aligning polyimide layers and solvent was slowly evaporated. Thin film of the polymer with embedded nanotubes was then heated, melted and covered with a top glass. The composite placed between two glass plates was oriented by rubbed polyimide coatings providing unidirectional orientation of the LC. Nanotubes had a tendency to aggregate during evaporation, but this tendency was overcome by sliding glass plates one with respect to the other. The distance between the glass plates was controlled by glass beads placed between the plates. The typical thickness of the samples was ~40 μm. The thickness of 40 μm was chosen because of consideration of several factors. The films with a smaller thickness were prone for spontaneous wrapping and folding after their detachment from the substrate, which made them very inconvenient for further manipulation. On the other hand in thicker films the orienting influence of the glass substrate is not transmitted through the whole film. The thickness of ~40 μm was therefore found to be the optimal as the films exhibited mechanical stability and satisfactory alignment of the nematic phase.

Polymerization of LCs was induced by UV lamp irradiation at 365 nm. Up to 20% of monomer may remain unpolymerized in highly cross-linked systems under UV polymerization conditions applied in this study. However, no traces of the monomer were found in DSC experiments. Moreover, the presence of the monomer should not influence the alignment of nanotubes since orientation of the latter occurs when the monomers are melted. The orientation achieved in the melted state is then almost instantly frozen in polymerization.

After polymerization, the upper glass was removed and polymer films with a low concentration of nanotubes were examined under the microscope in polarized light. The areas with the highest optical anisotropy were used for conductivity measurements and AFM imaging. The polymer films with a nanotube concentration higher than 4% were found to be completely opaque. The electrical conductivity of the composite films was measured by depositing silver microelectrode contact pads on the surface of composite films and using a

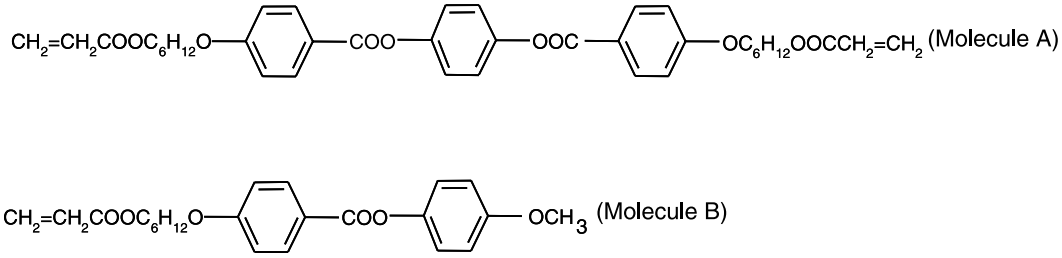

Scheme 1. Monomers used for LC polymer synthesis.

Keithley 2400 multimeter, which was operated by LabView software. A shadow masking technique was employed to deposit 100 nm thick microelectrode contacts with a gap of 200 μm between them. The contacts were deposited in the parallel and perpendicular directions to the LC orientation. The samples were characterized using a Raman spectrometer equipped with a He–Ne laser (excitation wavelength 632.8 nm). AFM imaging of the samples was performed in non-contact mode using Thermo Microscopes Autoprobe CP Research machine to reveal the orientation of the nanotubes in the composites.

3. Results and discussion

The morphology of the composites was studied using atomic force microscopy. Fig. 1(a) shows an AFM image of pristine SWNT on a silicon substrate. The average diameter of carbon nanotubes is ~1.4 nm (as estimated from cross-sections of AFM scans) with a length ranging from 5 to 10 μm. Also, as can be seen from Fig. 1(a), the nanotubes form bundles with a typical bundle diameter from 10 to 20 nm and length more than 10 μm. Fig. 1(b) shows the AFM image of the sample with 4% SWNT in the LC matrix as a typical example of nanocomposite morphology. The diameter of the elongated features on the AFM image agrees well with the measured average diameter of the SWNT bundles. The nanotubes are aligned along the LC director. The degree of alignment of the nanotubes deteriorated with increasing concentration. Fig. 1(c) shows the SEM image of the 6% SWNT sample and one can see the onset of the disruption of the orientation. This was more pronounced in the 10% SWNT composite, which exhibited almost isotropic distribution of nanotubes (Fig. 1(d)).

In our previous study, we have shown that the Raman spectra of LC polymer/nanotube composite films where the spectra of samples with different concentrations displayed a G band (arising due to the in-plane vibration of the C–C bonds) split into two components [13]. The G band of the 1% SWNT sample is 10 cm^{-1} right-shifted from the position of pristine nanotubes in accordance with the results discussed in [13]. Such a shift is indicative of the formation of fibrils and bundles embedded in the polymer matrix. In the present study, we address optical anisotropy of the composite samples with micro-Raman spectroscopy (the laser beam was focused into ~60 μm diameter spot on the sample surface) by monitoring the intensity of the SWNT G band depending on the angle between the polarization vector of the source and the nematic director (θ). The intensity of the G Raman bands of SWNT with polarized excitation was shown to be a good indicator of nanotubes' orientation [17]. We found that the anisotropy of G-band intensity was higher for the samples with smaller concentrations of SWNT and diminished as the concentration of nanotubes increased, this is shown in Fig. 2. The spectra at different angles were collected with the same experimental parameters except the change in the sample orientation. Fig. 2(a) and (b) shows the Raman spectra taken with different polarizations at two different angles (0 and 90°) for 1 and 10% concentration of SWNT respectively. The intensity of the G band peak exhibited a periodicity of 180° reaching a maximum

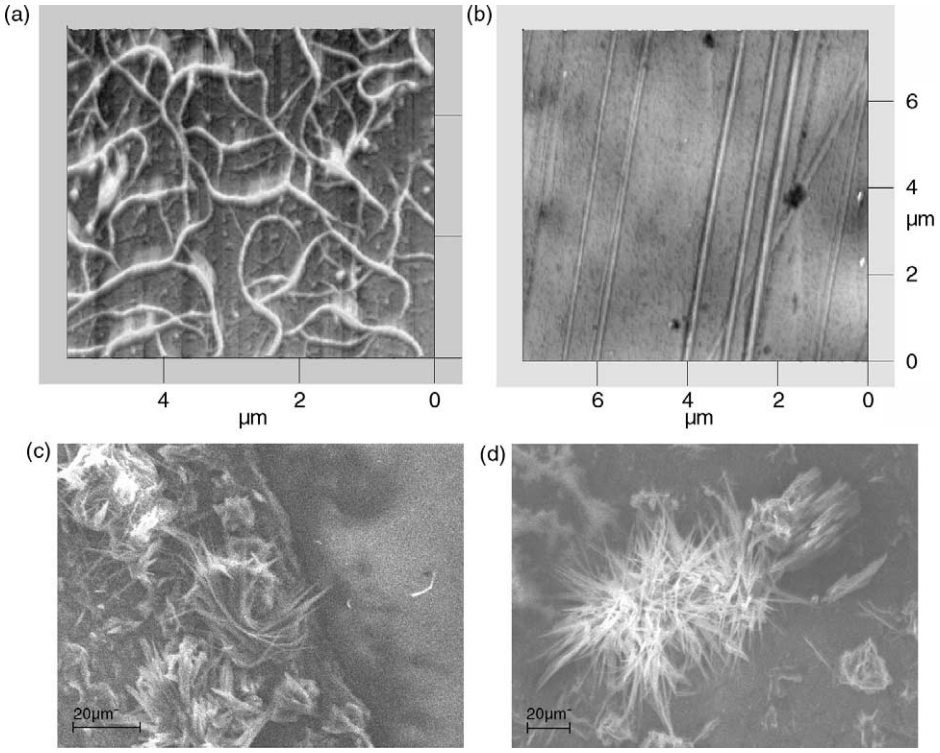

Fig. 1. Single walled carbon nanotubes (a) on silicon substrate randomly distributed depicting the bundled nature and average bundle diameter to be nearly 10 nm (b) aligned along the nematic vector in LC polymer matrix for 4% sample (c) in 6% sample showing the onset of distortion of the nematic order with high tendency to form bow-like structure (d) isotropic distribution in 10% sample.

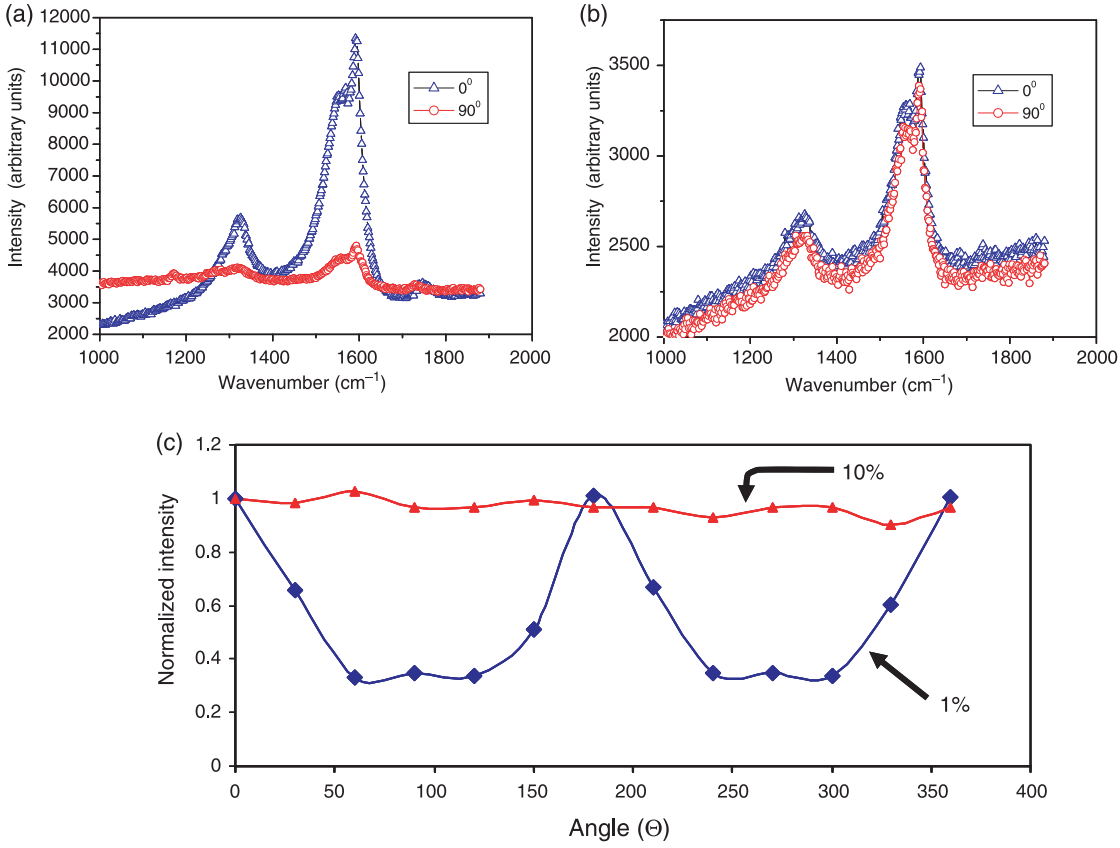

Fig. 2. Raman spectra of LC polymer/SWNT composites with 1% of SWNT (a) and of 10% of SWNT (b) for two different orientations of the film relative to the plane of light polarization. Strong dependence of the intensity of G band peak on the angle (θ) between the nematic director and the polarization vector is typical for small concentration of SWNTs (a) and is negligible for higher loads (b) (only two extreme cases of $\theta = 0$ and 90° are shown here), (c) dependence of the normalized intensity of the G peak on θ for 1 and 10% SWNT composites that demonstrates the anisotropic distribution of nanotubes for low concentrations of SWNT.

at $\theta = 0°$ and minimum at $\theta = 90°$ for low load samples (1% SWNT). On contrary, practically no variation of the G band intensity for different angles was detected for the spectra of 10% SWNT sample suggesting the nearly isotropic orientation of nanotubes in this composite film. Fig. 2(c) is a plot of the normalized intensity of the G band as a function of angle θ for 1 and 10% samples. The dependence of intensity on the orientation of sample corroborates the presence of preferential alignment of nanotubes along the nematic director in 1% samples and the absence of one in 10% samples. Therefore, the isotropic orientation of nanotubes in composite films prevails in high load samples.

Highly anisotropic distribution of nanotubes in the polymer matrix was also confirmed by measuring the electrical conductivity in the directions perpendicular and parallel to the orientation of the nematic LC. Fig. 3 summarizes the main features of the polymers' conductivity measured at different concentrations of nanotubes. Fig. 3(a) shows the typical behavior for the current density of a composite (6% of SWNT) for two configurations of the contacts with their longest sides oriented in parallel (transverse) and perpendicular (longitudinal) directions to the LC alignment. The comparison between different samples and different orientations was made by accounting for the size of the electrodes and the gap between them (Fig. 3(b)). The conductivity of polymer composites varies with the concentration of nanotubes. At low concentrations of nanotubes, the current density in the direction parallel to the orientation of a nematic polymer is much higher than in the perpendicular direction. The anisotropy of conductivity also depends on the nanotubes' concentration. The highest anisotropy of current density was observed for the lowest concentration (1%) of SWNT. The current density in the direction parallel to the orientation of the LC was almost three orders of magnitude higher as compared to the one in the perpendicular direction. Interestingly, the conductivity in large samples (20 mm) measured in two perpendicular directions differs only by a factor of two. Anisotropy of conductivity decreases with increasing concentration of the filler. For a sample with 6% of SWNT the current density in the longitudinal direction was only two orders of magnitude higher compared to the transverse direction. The anisotropy of conductivity completely vanished for the sample with 10% SWNT.

There are contradictory literature data on the percolation threshold in polymer systems containing SWNT. In accordance to [18] the percolation threshold for SWNT dispersed in polyparaphenylvynilene is less than 2%. In [19] the percolation threshold in the composite with a similar polymer was determined to be 8.5%. Our results shed some light on the nature of the discrepancy between different studies that is most likely the result of different orientation of nanotubes inside the

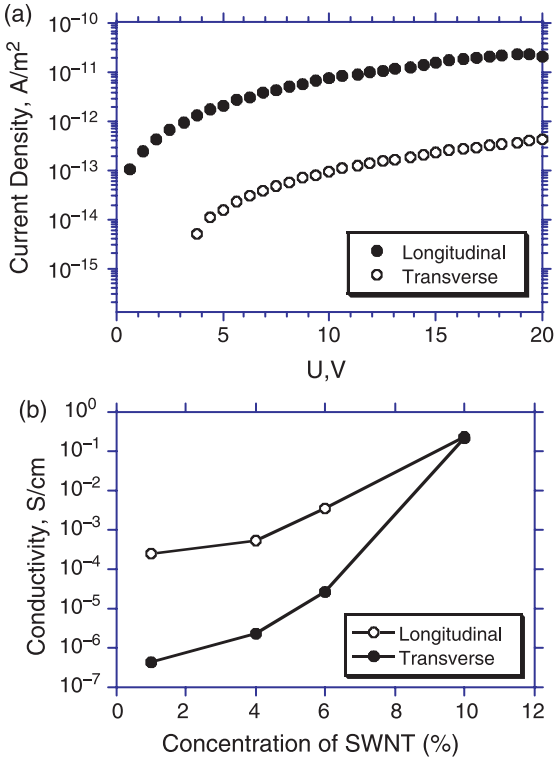

Fig. 3. (a) Semi logarithmic plot of *I–V* behavior of sample with 6% SWNT depicting a nearly two orders of magnitude difference in the electrical conductivity between transverse and longitudinal directions, (b) summary of the *I–V* behavior of the LC–SWNT composite samples at various concentrations showing a diminishing anisotropy with increasing concentration.

sample with respect to the electric contacts and nanotubes' aggregation depending on the nature of the polymer matrix.

The percolation threshold also depends on the ratio between the average length of the formed nanotube bundles and the distance between contacts (in the following text our reference to the nanotubes also means the bundles which they usually form). First, let us consider how the average length of the nanotubes (L) and the width of the contact gap (G) determine the conductivity of the samples with different orientations of nanotubes. In case of almost ideal orientation of nanotubes lying in the direction perpendicular to the contacts (Fig. 4(a)) the increase in the ratio L/G results in increasing conductivity and lowering of the percolation threshold since more and more bundles start to form contacts with electrodes. However, in the direction parallel to the contacts (Fig. 4(b)) the same sample may not be conductive at all, since bundles do not form electric contacts with the electrodes and conductivity of the composite will be determined by the effective hopping length. When the distance between contacts increases the difference between these two cases diminishes. In the limit $L \ll G$ the percolation threshold will be determined by the concentration of bundles, not their length [20]. When the distribution of nanotubes becomes less anisotropic the conductivity of samples with electrodes parallel to the director becomes almost the same as the conductivity of the samples with electrodes perpendicular to the director.

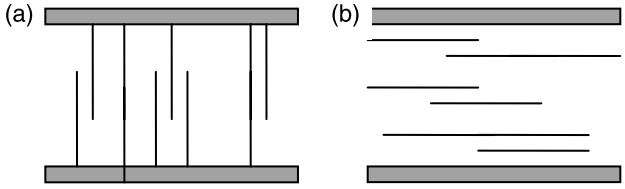

Fig. 4. The alignment of carbon nanotubes perpendicular and parallel to the electrodes in longitudinal and transverse directions, respectively.

In real polymer matrices the orientation of nanotubes is never ideal. We propose the following semi-quantitative model describing the orientation and conductivity of nanotubes in oriented LC polymers when L is comparable to G.

Following [20,21] we assume that the average length of the bundles is simply defined by the following equation $L = \sum_i L_i/N$. In our model all nanotubes have the same length L, half of them are oriented at angles ϑ_0 and the other half at angles $-\vartheta_0$ with respect to the axis perpendicular to the contacts (Fig. 5). There is also a uniform angular distribution around the angles ϑ_0 defined by the angular width $\Delta\vartheta$. Let us now look at a cluster propagating from the lower contact towards the upper. The probability that nanotubes form a percolating cluster is defined by a product

$$P = P_a \prod_{j=1}^{M} P_{j,j-1} \tag{1}$$

where P_a is the probability that two nanotubes have electrical contacts with two electrodes, P_j is the probability that two nanotubes numbered j and $j-1$ are electrically connected (simply intersect) and M is the number of nanotubes in a cluster. The conductivity of the sample is proportional to P. When the electrical contact of length A is deposited on the polymer the probability per unit length that it intersects any nanotube is simply proportional to the half of the component of the nanotube length in the direction perpendicular to the contact, for two contacts $P_a = L\cos(\vartheta)n$ where n is the two-dimensional concentration of nanotubes' centers $n = N/AG$. Suppose, we have started at the low contact and now look at the j-th nanotube belonging to the percolating cluster and oriented at an angle $-\vartheta_0$ above the lower contact. Since the width of the

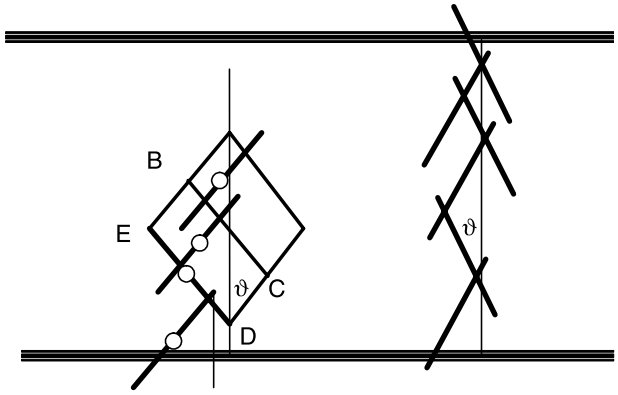

Fig. 5. Structure of a growing model cluster (at left) and percolating cluster (at right).

angular distribution $\Delta\vartheta$ is small we suppose that nanotubes oriented at the same angles almost do not intersect. The only nanotubes able to intersect with the nanotube j are those oriented at the angles $-\vartheta_0$. The centers of these nanotubes must lie in the area BCDE in Fig. 5 which is in accordance to Balberg [20] we will call an excluded area of two nanotubes. The probability to find j nanotube belonging to the excluded area is

$$P_{j,j+1} = \frac{L^2 \sin(\vartheta_j + \vartheta_{j+1}) \cos(\vartheta_j + \vartheta_{j+1})(M-j)}{S_{\text{tot}}} \tag{2}$$

where S_{tot} is a total area available for the nanotube. Here we are interested in studying the angular dependence of P rather than in detailed evaluation of P. We will calculate the average probabilities P_{a} and $P_{j,j-1}$ by using distribution function $f(\vartheta)$:

$$f(\vartheta) = \begin{cases} 1, & \vartheta_0 < \vartheta < \vartheta_0 + \Delta\vartheta \\ 0, & \vartheta < \vartheta_0, \vartheta > \vartheta_0 + \Delta\vartheta \end{cases} \tag{3}$$

After integration of Eq. (2) we will get:

$$\langle P_{j,j+1} \rangle \cong \frac{2\sin(2\vartheta_0 + \Delta\vartheta) - \sin(2(\vartheta_0 + \Delta\vartheta)) - \sin(2\vartheta_0)}{\Delta\vartheta} \times L^2(M-j), \tag{4a}$$

$$\langle P_{\text{a}} \rangle \cong \frac{\sin(\vartheta_0 + \Delta\vartheta) - \sin(\vartheta_0)}{\Delta\vartheta} Ln \tag{4b}$$

If nanotubes are aligned predominantly parallel to the director then their orientation is defined by the angle $\vartheta = \vartheta_{\text{par}} < 45°$. If nanotubes are aligned predominantly perpendicular to the director then the angle $\vartheta = \vartheta_{\text{perp}} > 45°$. Isotropic orientation corresponds to $\vartheta_0 = 45°$. The ratio between conductivity in the direction parallel to the alignment of nanotubes and conductivity in the perpendicular direction is given by:

$$\frac{I_{\text{par}}}{I_{\text{perp}}} = \frac{\sin(\vartheta_{\text{par}} + \Delta\vartheta) - \sin(\vartheta_{\text{par}})}{\sin(\vartheta_{\text{perp}} + \Delta\vartheta) - \sin(\vartheta_{\text{perp}})} \times \left(\frac{2\sin(2\vartheta_{\text{par}} + \Delta\vartheta) - \sin(2(\vartheta_{\text{par}} + \Delta\vartheta)) - \sin(2\vartheta_{\text{par}})}{2\sin(2\vartheta_{\text{par}} + \Delta\vartheta) - \sin(2(\vartheta_{\text{perp}} + \Delta\vartheta)) - \sin(2\vartheta_{\text{perp}})} \right)^M \tag{5}$$

It is important to note that Eq. (5) can be used only to estimate the ratio of parallel and perpendicular conductivities above the percolation threshold, which for the samples with L comparable to G depends on the orientation of nanotubes. The minimum number of nanotubes forming a percolating cluster can be simply estimated as $M = G/L = 20$; we used this number to calculate a ratio of conductivity as a function of their orientation.

Our model predicts dramatic changes in the ratio $I_{\text{par}}/I_{\text{perp}}$ as the angle ϑ increases. Very sharp changes occur in the range $0° < \vartheta < 25°$. Experimentally measured anisotropy of conductivity and theoretical calculations based on Eq. (5) are plotted together in Fig. 6. In this figure we try to establish a relationship between concentration of nanotubes and average orientation defined by an angle ϑ. This mapping helps to realize what influence the increase in concentration of nanotubes has on the angle ϑ and conductivity. At the angle $\vartheta = 45°$ no anisotropy exists in the film. This means that components of the vector defined by the nanotube on the directions parallel and perpendicular to the contacts are the same (Fig. 5). Our experimental data show that this point corresponds to a concentration of 10%. At smaller concentrations of nanotubes and consequently smaller angles the anisotropy of the conductivity increases. Of course, our model does not consider the cause of the changes of the angular distribution of nanotubes. It just attempts to quantify the ratio of conductivity in two perpendicular directions when the changes in the nanotube orientation have already occurred. The similarity in the behavior of the two curves not only justifies the mapping but also permits us to draw conclusions about the orientation of nanotubes at lower concentration.

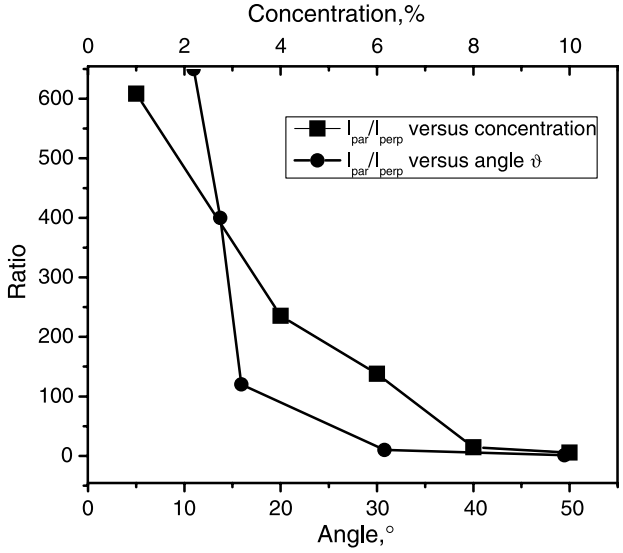

Fig. 6. Conductivity ratio in the directions parallel and perpendicular to the alignment versus the average angle (ϑ) of nanotubes orientation (calculations based on Eq. (5)) and the concentration of nanotubes (experimental data).

At relatively low nanotube concentration, when they practically do not interact with each other, their alignment is governed by the LC matrix. The anchoring angle of LC molecules on the surface of nanotubes is close to the angle between the LC molecules and graphite surface (about $\theta = 12°$) [22]. These boundary conditions as well as the shape of the nanotube bundles create a distortion of the nematic field around carbon nanotubes and bundles, which results in the appearance of nematic defects around them. At low concentrations of nanotubes the nematic field is not significantly disturbed and relaxes back to the planar orientation imposed by the glass plates at a length scale much smaller than the distance between the nanotubes. The distortion energy induced in the nematic phase depends on the orientation of nanotubes like $F \approx 2\pi KL\theta^2$ where θ is the angle between the long axis of the nanotube and nematic director, K is the elastic constant of the nematic matrix. The higher this angle, the larger the distortion energy F [23] induced by a single nanotube. If a second nanotube

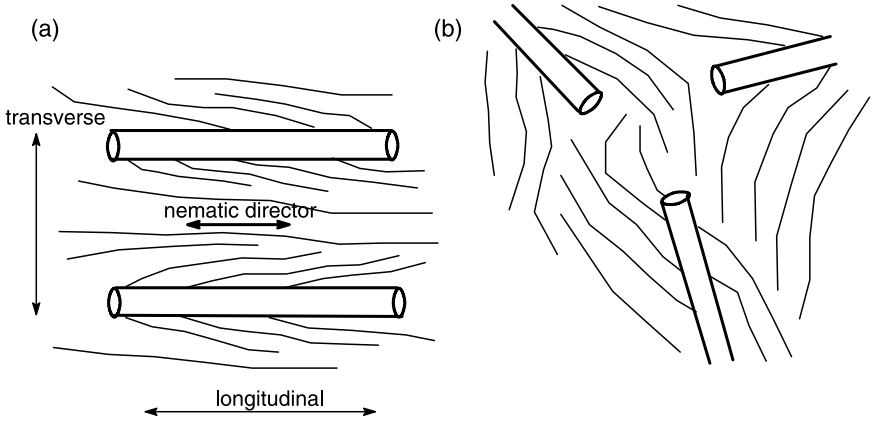

Fig. 7. Ordered nanotubes and nematic director in case of low concentrations of nanotubes (a) and isotropic distribution at higher concentrations (b).

happens to be in the area of the distorted nematic it will also give rise to an increase in distortion energy and therefore will experience less orienting torque from the nematic matrix. This process is 'self-accelerating': The more nanotubes in the matrix the less orienting influence they feel from the matrix. Therefore, when the concentration of nanotubes reaches a certain threshold there will be no ordered nanotubes. When the concentration of nanotubes is relatively low the LC order of the polymer matrix is obeyed also by the nanotubes as schematically shown in Fig. 7(a). At these low concentrations a percolation as well as an electrical conductivity below and above the percolation threshold are much smaller in the directions perpendicular to the nanotubes. In the latter case the nanotubes are separated by nonconductive polymer matrix, which makes the percolation threshold higher. When concentration of nanotubes rises the nematic order is locally destroyed (Fig. 7(b)). Aggregates of nanotubes are formed as shown in Fig. 1(d) and the degree of anisotropy vanishes. The orientation of nanotubes and their bundles is not governed any longer by the interaction with the nematic matrix, but depends on the interaction of nanotubes with each other. The number of direct contacts between nanotubes increases and distortion of the nematic matrix rises with increasing concentration of nanotubes. The entanglements between nanotubes and their bundles provide a complex, confining geometry with severely distorted nematic order observed in recent studies of dense packed colloidal particles [24].

4. Conclusions

SWNTs have been aligned along the nematic vector direction in a liquid crystalline polymer matrix. The alignment is confirmed by AFM imaging and by the observed anisotropy of electrical conductivity and Raman spectra of the composite films. The degree of alignment varies with the concentration of carbon nanotubes. The alignment is high for relatively low concentrations (up to 4%), gradually fades as the concentration increases and finally vanishes at 10% of nanotubes. A simple semi-quantitative model is proposed to explain the underlying mechanism of alignment and its dependence on the concentration of nanotubes.

Acknowledgements

P.V.S. appreciates the support from Fordham Research Grant Program, Fordham Alumni Fund, the US Civilian Research and Development Foundation (grant#GEP2-2648-TB05) and Donors of the Petroleum Research Fund of American Chemical Society. V.N.B. thanks support for this work from the Faculty Research and Creative Activity Support Fund, Western Michigan University.

References

[1] Thostenson ET, Ren Z, Chou T. Compos Sci Technol 2001;61:1899.
[2] Breuer O, Sundararaj U. Polym Compos 2004;25:630.
[3] Lau K, Hui D. Composites, Part B 2002;33:263.
[4] Bliznyuk VN, Baig A, Singamaneni S, Pud AA, Fatyeyeva KY, Shapoval GS. Polymer 2005;46:11728.
[5] Foster J, Singamaneni S, Kattumenu R, Bliznyuk V. Colloids Interface Sci 2005;287:167.
[6] Gao J, Itkis ME, Yu A, Bekyarova E, Zhao B, Haddon RC. J Am Chem Soc 2005;127:3847.
[7] Dierking I, Scalia G, Morales P, LeClere D. Adv Mater 2004;16:865.
[8] Kimura T, Ago H, Tobita M, Ohshima S, Kyotani M, Yumura M. Adv Mater 2002;14:1380.
[9] Jin L, Bower C, Zhou O. Appl Phys Lett 1998;73:1197.
[10] Hobbie EK, Wang H, Kim H, Lin-Gibson S, Grulke EA. Phys Fluids 2003;15:1196.
[11] Ko H, Peleshanko S, Tsukruk VV. J Phys Chem B 2004;108:4385.
[12] Shim BS, Kotov NA. Langmuir 2005;21:9381.
[13] Bliznyuk V, Singamaneni S, Sanford RL, Chiappetta D, Crooker B, Shibaev PV. J Nanosci Nanotechnol 2005;5:1651.
[14] Du F, Fischer JE, Winey KI. Phys Rev B 2005;72:121404.
[15] Cadek M, Coleman JN, Barron V, Hedicke K, Blau WJ. Appl Phys Lett 2002;81:5123.
[16] Shibaev PV, Madsen J, Genack AZ. Chem Mater 2004;16:1397.
[17] Fischer JE, Zhou W, Vavro J, Llaguno MC, Guthy C, Haggenmueller R, et al. J Appl Phys 2003;93:2157.
[18] Mulazzi E, Perego R, Aarab H, Mihut L, Lefrant S, Faulques E, et al. Phys Rev B 2004;70:155206.
[19] Coleman JN, Curran S, Dalton AB, Davey AP, McCarthy B, Blau W, et al. Phys Rev B 1998;58:R7492.
[20] Balberg I, Anderson CH, Alexander S, Wagner N. Phys Rev B 1984;30:3933.
[21] Boudville WJ, McGill TC. Phys Rev B 1989;39:369.
[22] Mongous JD, Brackley AJ, Foland K, Baker RT, Patrick DL. Phys Rev Lett 2000;84:2742.
[23] De Gennes PG. J Phys 1970;31:691.
[24] Meeker SP, Poon WCK, Crain J, Terentjev EM. Phys Rev E 2000;61:R6083.